UCLA
COMPUTATIONAL AND APPLIED MATHEMATICS

A Level-Set and Gabor-Based Active Contour Algorithm for Segmenting Textured Images

Berta Sandberg
Tony Chan
Luminita Vese

July 2002

CAM Report 02-39

Department of Mathematics
University of California, Los Angeles
Los Angeles, CA. 90095-1555

http://www.math.ucla.edu/applied/cam/index.html

A Level-Set and Gabor-based Active Contour Algorithm for Segmenting Textured Images *

Berta Sandberg

Mathematics Dept.
UCLA
405 Hilgard Avenue
Los Angeles CA 90095
U.S.A.
bsand@math.ucla.edu

Tony Chan

Mathematics Dept.
UCLA
405 Hilgard Avenue
Los Angeles CA 90095
U.S.A.
lvese@math.ucla.edu

Luminita Vese

Mathematics Dept.
UCLA
405 Hilgard Avenu
Los Angeles CA 900
U.S.A.
chan@math.ucla.ed

Abstract

This paper applies the authors' previously proposed vector valued active contour without edges model to segment textured images. The model uses a level set implementation and can detect edges without the use of gradient information, making it natural for use in textured image segmentation. Multiple Gabor transforms of the original image are used to discriminate textures. We show numerical results for segmentation and discrimination of textures, using supervised and unsupervised forms of the model.

1 Introduction

When looking at a textured image, the human eye has to look a little harder in order to spot the different textures. Likewise, when using a computer to segment the image, we need to change the standard segmentation models to allow the computer to segment the textured image. There are several problems specific to texture segmentation: when the textures have the same intensities, it is very difficult for the standard segmentation models to tell them apart; another problem inherent in textured segmentation is that it is often difficult to pick out the boundary between two textures because there is no sharp difference between them. Finally, any texture segmentation algorithm should be robust to noise, since texture has small patterns that are "noise" like.

A vector-valued active contour and segmentation model could be a way for overcoming these three problems, all together. Most active contour models and segmentation algorithms use the gradient of the image in their edge detectors, but then as a result unclear boundaries between two textures are hard to be detected. These models need in addition to perform a-priori smoothing, to smooth out the noise. This can therefore produce a not very accurate location of edges. Among the classical models for active contours based on a gradient-edge-function for the stopping criteria, we mention [12], [4], [15], [5], [13], [15], [32], [26], [19].

The active contour and segmentation model used in this paper [36], [37] does not use the gradient to detect boundaries. This property allows the model to be robust to noise, and to segment color and multi-spectral images where there are no clear gradient-boundaries. It is based on the piecewise-constant Mumford and Shah model for segmentation [17], and it uses the level set method [18] for the representation of the evolving contour. In addition, it does not need an a-priori smoothing of the image, and therefore edges are much better located.

We propose here a natural extension of [37] to textured images since these images often cannot be segmented using the gradient as an edge detector. In addition, the model from [37] and [36] allows for automatic detection of interior contours, detection of edges which cannot be defined by gradient, without using an a-priori smoothing. These advantages could not be obtained by the previous active contour models, such as [12], [4], [15], [5], [13], [15], [32], [26], [19].

For the texture discrimination, we propose to use Gabor functions, having properties similar to those of early visual channels, being localized in space and frequency domains [10], [6]. Here, we convolve the Gabor functions with the original textured image to obtain different channels. Some of these channels will be the input of the multi-channel active contour algorithm.

To summarize, in this paper we propose a combined framework of the vector-valued active contour model without edges from [37] and Gabor functions, to segment tex-

*This work has been supported in part by grants ONR N00014-02-1-0015, NIH P20MH65166, NSF ITR-0113439, and NSF DMS-9973341.

tured images. This paper is closely related with [19] and [20], where the Gabor function is also used to discriminate textures, in a curve evolution based probabilistic approach. In these works, it is assumed that a texture pattern is given [19] (called preferable texture pattern), or that a set of texture patterns are known a-priori [20]. It is also assumed there that an a priori knowledge about the desired intensity properties of the different regions is available.

Here, we do not assume any a-priori knowledge or statistical information on the type of textures, or on the type of intensity, or on the location of boundaries. The proposed model here is quite general, and it can be applied in many situations. In addition, the vector-valued active contour model from [37] can recover a full object from combined channels of the same image, even if there are missing parts in some of the channels. As we will see in the numerical results, this property is very appropriate and useful in recovering objects filtered by several Gabor functions.

Other transforms could be used of course, instead of the Gabor transform, for texture discrimination, such as wavelets (see for example [21]).

This paper is related to many other works on active contours and texture segmentation, such as [19], [20] (already mentioned above), [27], [28], [29], [23], [14]. Additional related papers are [16], [40], [41], [42].

Other related works on segmentation, edge-preserving smoothing, and vector-valued images (e.g. multi-channels, color, etc), are [7], [14], [22], [24], [25], [34], [35].

2 Description of the model

We begin by recalling the Gabor function and the vector-valued active contour model without edges from [37].

2.1 The Gabor function

In this section, we review the basics of the Gabor transforms necessary for our model. The 1-D Gabor function was first defined by Gabor [8], and later extended to 2-D by Daugman [6].

The Gabor function has often been implemented in texture segmentation because it is similar to a biological vision system which is localized in space and frequency. It has the property that it can segment images having region differences in spatial frequency, density of elements, orientation, phase, and energy, as explained in [3].

A 2-D Gabor filter is an oriented complex sinusoidal grating modulated by a 2-D Gaussian function, which is given by

$$G_{\sigma,F,\theta}(x,y) = g_\sigma(x,y)\exp[2\pi jF(x\cos\theta + y\sin\theta)], \quad (1)$$

where

$$g_\sigma(x,y) = \frac{1}{2\pi\sigma^2}\exp[-\frac{x^2+y^2}{2\sigma^2}].$$

Note that we use the notation j for the complex number i. The frequency of the span-limited sinusoidal grating is given by F and its orientation is specified as θ; σ is a scale parameter. The parameters of a Gabor filter are therefore given by the frequency F, the orientation θ, and the scale σ. The Gabor filter $G_{\sigma,F,\theta}$ gives a complex-valued function, decomposed by $G_{\sigma,F,\theta} = G_R + jG_I$ into real and imaginary parts.

Giving an image function u_0, defined on a planar domain Ω, and taking real values, we can convolve it with the Gabor function, to obtain Gabor transforms of u_0:

$$(u_0)_{\sigma,F,\theta} = \sqrt{(G_R * u_0)^2 + (G_I * u_0)^2}.$$

We vary F, θ, σ, to obtain different input channels for the active contour model for vector-valued images. We normalize the channels between 0 and 255.

2.2 Multi-Channel Model

Here we give the details of the multi-channel active contour model without edges from [37], based on Mumford and Shah segmentation [17] and the level set method [18].

Let u_0 be the textured image, defined on a planar domain Ω with real values (for simplicity only, but color texture segmentation could also be considered). Let u_0^i, for $i = 1, ..., N$, be N Gabor transforms of the original image u_0, obtained for different parameters (F, θ, σ). These will be the channels or entries in the multi-valued active contour model.

Let C be the evolving contour. Each channel being a different transform of the same image u_0, we denote by c_+^i and c_-^i the two averages of u_0^i inside and outside the curve C, respectively, for $i = 1, 2, ..., N$. Following [37], the following energy was introduced, which, when minimized with respect to $\overline{c_+} = (c_+^1, ..., c_+^N)$, $\overline{c_-} = (c_-^1, ..., c_-^N)$, and C, performs active contours, denoising and binary segmentation:

$$E(C, \overline{c_+}, \overline{c_-}) = \mu \cdot \text{length}(C) +$$
$$\int_{inside(C)} \frac{1}{N}\sum_{i=1}^{N} \lambda_i |u_0^i(x,y) - c_+^i|^2 dxdy +$$
$$\int_{outside(C)} \frac{1}{N}\sum_{i=1}^{N} \gamma_i |u_0^i(x,y) - c_-^i|^2 dxdy.$$

The positive scalars λ_i and γ_i, for $i = 1, ..., N$ are weight parameters for each channel. Minimizing the above energy, one tries to segment possible objects in the image with contours given by C and represented by the region "inside C", from a uniform background represented by the region "outside C".

In [37], the implementation has been done using the level set method of S. Osher and J. Sethian [18], which gives an efficient method for moving curves and surfaces, on a fixed regular grid, allowing for automatic topology changes, such as merging and breaking of curves etc. The curve C is represented implicitly, via a level set function ϕ, such that $C = \{(x,y) : \phi(x,y) = 0\}$, and $\phi(x,y) > 0$ inside C, $\phi(x,y) < 0$ outside C.

Following [33] and [36], the above energy is then expressed in the level set formulation as follows. We recall the Heaviside function H to be defined as:

$$H(x) = \begin{cases} 1 & \text{if } x \geq 0, \\ 0 & \text{if } x < 0, \end{cases}$$

and the Dirac Delta function $\delta(x) = \frac{d}{dx}H(x)$, in the sense of distributions. Then, rewriting E in level set form, we obtain:

$$E(\phi, \overline{c_+}, \overline{c_-}) = \mu \int_\Omega \delta(\phi)|\nabla\phi| dxdy +$$
$$\int_\Omega \frac{1}{N}\sum_{i=1}^{N} \lambda_i |u_0{}^i(x,y) - c_+^i|^2 H(\phi) dxdy +$$
$$\int_\Omega \frac{1}{N}\sum_{i=1}^{N} \gamma_i |u_0{}^i(x,y) - c_-^i|^2 (1 - H(\phi)) dxdy.$$

Minimizing the above energy with respect to the unknown constant vectors $\overline{c_+}$ and $\overline{c_-}$, we obtain the following relations, embedded in a time-dependent scheme:

$$\begin{aligned} c_+^i(t) &= \frac{\int_\Omega u_0^i H(\phi) dxdy}{\int_\Omega H(\phi) dxdy}, \\ c_-^i(t) &= \frac{\int_\Omega u_0^i (1 - H(\phi)) dxdy}{\int \Omega H(\phi) dxdy}, \end{aligned}$$

i.e. the averages of channels u_0^i inside and outside the curve C respectively, for $i = 1, 2, ..., N$, where N is the number of channels.

Minimizing the above energy with respect to ϕ, and parameterizing the descent direction by an artificial time, we obtain the following Euler-Lagrange equation for ϕ:

$$\begin{cases} \phi(0,x,y) = \phi_0(x,y), \\ \frac{\partial\phi}{\partial t} = \delta_\epsilon(\phi)[div(\frac{\nabla\phi}{|\nabla\phi|} - \mu - \frac{1}{N}\sum_{i=1}^{N}\lambda_i(u_0^i - c_+^i)^2 \\ +\frac{1}{N}\sum_{i=1}^{N}\gamma_i(u_0^i - c_-^i)^2] \text{ in } \Omega, \\ \frac{\delta_\epsilon(\phi)}{|\nabla\phi|}\frac{\partial\phi}{\partial\vec{n}} = 0 \text{ on } \partial\Omega, \end{cases}$$

where we have regularized the Heaviside function H by a smooth approximation H_ϵ, as $\epsilon \to 0$, as in [36], [37], and $\delta_\epsilon = H'_\epsilon$.

Starting with an initial contour, given by ϕ_0, at each time step we update the vector averages $\overline{c_+}$ and $\overline{c_-}$, and we evolve the PDE in ϕ.

The obtained model detects contours both with or without gradient, interior contours automatically, and is robust to noise. The initial contour can be placed anywhere, not necessarily completely enclosing the objects to be detected.

3 Experimental Results

In order to segment the textured image, we first convolve the image with different Gabor functions. We have found that the following parameters give satisfactory results: $\theta = \{0, \pi/6, \pi/4, \pi/3, \pi/2\}, F = \{60, 90, 120\}$ (of a 256x256 image) and $\sigma = \{.0075, .005, .0025\}$ (see also [9]). Using all the combinations of the parameters, we obtain 45 different images as possible channels. Using all of these channels for segmentation is cumbersome, especially as some of the images are redundant while others do not help in detection. Also, when we use all the possible transforms the computation time will be longer, and it may not give the desired result due to conflicting information.

At this point we divide our model into two parts: "supervised" texture segmentation, when the user chooses the "best" Gabor transforms, to be used as input channels; and "unsupervised" texture segmentation, where the Gabor transforms to be used are chosen by a dynamic automatic criterion.

The case of supervised texture segmentation allows to use fewest number of transforms in order to segment the image, and as a result it does a very good job, with optimal computational efficiency.

The case of unsupervised texture segmentation is similar to the work of [11], [31]. The criterion that we used for the automatic choice of the Gabor transforms is based on the following: we want the images to have the highest intensity differences relative to the mean of the image. Thus for each transformed channel i we calculate the following:

$$s_i = |c_i^+ - c_i^-|.$$

Only n channels corresponding to the first n largest values of s_i are used in our active contour model as inputs, at the initial time and at later times. Using this criterion may require more channels to be chosen than in the supervised case, because not all the picks are good, however this criterion does a fair job of picking out automatically the "best" channels. Then, we update the chosen transforms by this criterion every 10-100 iterations. At every test, we have the same number of transforms which will be used, for the same experiment, but these transforms may dynamically change.

The following experimental results are presented. Each figure shows the original textured image, the final segmentation, followed by a sampling of the Gabor transforms (in some examples, we also show the evolution of the contour). In the unsupervised case, we show the final n channels issued from the automatic criterion.

While the Gabor transforms have more intensity contrast, thus clearer edges then the original images, there is still a lot of detail texture in them. By picking the proper parameters, our Gabor-based active contour model is able to segment the textured image.

We denote by $\overline{\lambda} = (\lambda_1, ..., \lambda_N)$, and $\overline{\gamma} = (\gamma_1, ..., \gamma_N)$. If $\overline{\lambda} > \overline{\gamma}$, it forces the contour to decrease, this is necessary as there is a lot of patterns in the object and the model favors encompassing all of them rather than finding the largest object. The large μ allows the model to ignore small patterns which still show in the Gabor transforms.

In Figure 1, there is a square in the middle of the image, but it is very hard to distinguish it. The Gabor transforms contrast the square, with the outside texture, and the active contour model has no problem detecting the edges of the square.

In Figure 2, a texture is oriented at 90 degrees to itself. Again we find that the model segments between the different orientations. In these first two examples, we use the supervised choice of the Gabor transforms.

In Figure 3, we have a texture image with noise. Despite the fact that the Gabor transforms were noticebly worse, the model was still able to pick out the square object.

In Figure 4, we have an example of when the model does not work. In this example we have a brick wall, and another brick wall slightly staggared. The human eye can see it clearly. However the Gabor transforms are not able to differentiate between the two objects well since it's the same texture at the same angle. The model is not able to find the boundary between the objects in this case.

In Figures 5 and 6, we consider the same images from Figures 1 and 2, but this time we use the unsupervised version of the model. It is still able to correctly segment the images, even though some of the channels do not extract the desired information.

In Figure 7, we have an example of a more complicated textured image of two zebras. The supervised model segments the image well by discriminating the bodies from the shadow and the background. Note that interior contours are detected by the level set active contour model (under the head of the larger zebra).

In Figures 8 and 9, we have used the unsupervised criteria for choosing the Gabor transforms (we have four and eight channels respectively). Notice that details are missing from both sets of transforms, but the obtained results are very satisfactory. With the eight channels, some smaller details are lost, compared with the supervised texture segmentation from Figure 7.

Note that, even if the original textured images have "clear" boundaries that human can perceive, in the Gabor transforms, these boundaries are sometimes still very fuzzy or blurred (see for example Figure 3 channel 2, or Figure 5 first two channels), and therefore these illustrates the need of a model that can handle smooth boundaries. The active contour model used here is very appropriate, because it does not use the gradient as an edge detector, like in other more classical models. In addition, discontinuous edges with missing parts are very well recovered (as illustrated in Figure 7).

4 Concluding remarks

In this paper, we have proposed a level set and Gabor-based active contour model for segmenting textured images. For the purpose of illustration, we have considered here only the case of images with two textures. The general case, with more than two textures to be segmented, can easily be considered, in the same framework, by using the multi-phase level set segmentation models from [39] and [38], combined with the Gabor transform, in a multi-channel framework.

References

[1] J.M.H. du Buf and P. Heitkamper, "Texture features based on Gabor Phase", Signal Processing Vol. 23, pp. 227-244, 1991.

[2] P. Burt and E.H. Adelson, "The Laplacian Pyramid as a Compact Image Code", IEEE Transactions on Communication COM, Vol 31, pp. 532-540, 1983.

[3] M. Clark and A. C. Bovik, Wilson S. Geisler, "Multichannel Texture Analysis Using Localized Spatial Filters", Transactions on Pattern Analysis and Machine Intelligence, Vol. 12, No. 1, pp. 55-73, 1990.

[4] V. Caselles, F. Catté, T. Coll and F. Dibos, "A geometric model for active contours in image processing", Num. Math., Vol. 66, 1-31, 1993.

[5] V. Caselles, R. Kimmel and G. Sapiro, "On geodesic active contours", Int. J. of Computer Vision, Vol. 22/1, pp. 61-79, 1997.

[6] J. G. Daugman, "Uncertainty relation for resolution in space, spatial frequency, and orientation optimized by two-dimensional visual cortical filter", J. Opt. Soc. Am. A, Vol. 2/7, pp. 1160-1169, 1985.

[7] F. Dibos and G. Koepfler, "Color segmentation using a variational formulation", Actes du 16me Colloque GRETSI, Grenoble, pp. 367-370, 1997.

[8] D. Gabor, "Theory of communication", Journal of the Institute of Electrical Engineers, Vol. 93, pp. 429-457, 1946.

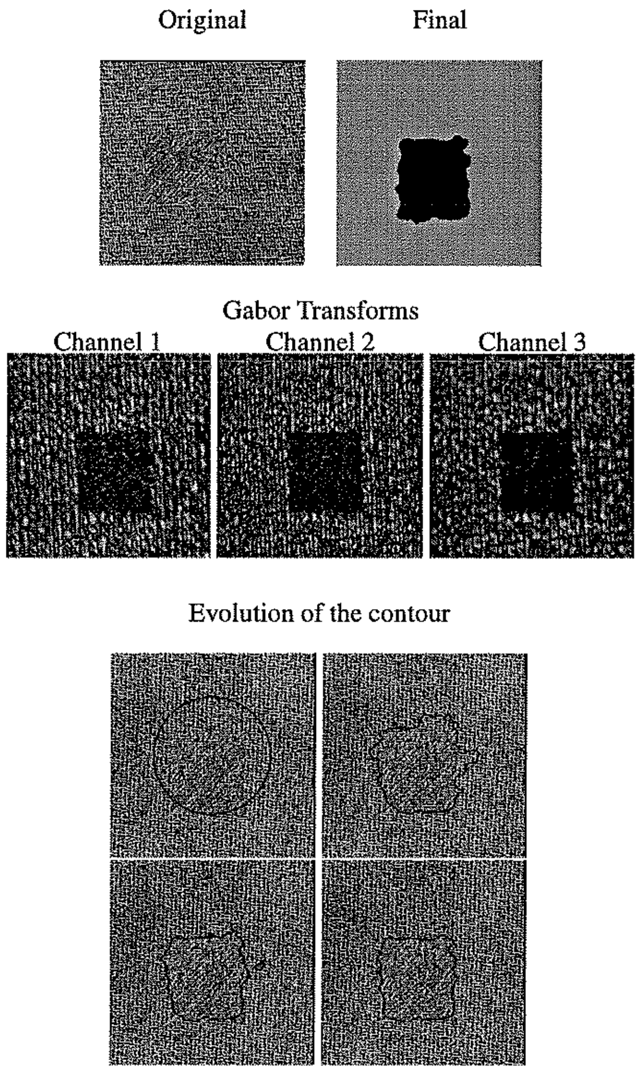

Figure 1: Supervised model with three different Gabor transforms as input channels. Parameters: $\lambda_i = 1$, $\mu = 4000$, $\gamma_i = .3$. The boundary of the full square is found, and the binary segmentation is represented by "gray" and "black" ("black" if $\phi \geq 0$, and "gray" if $\phi < 0$).

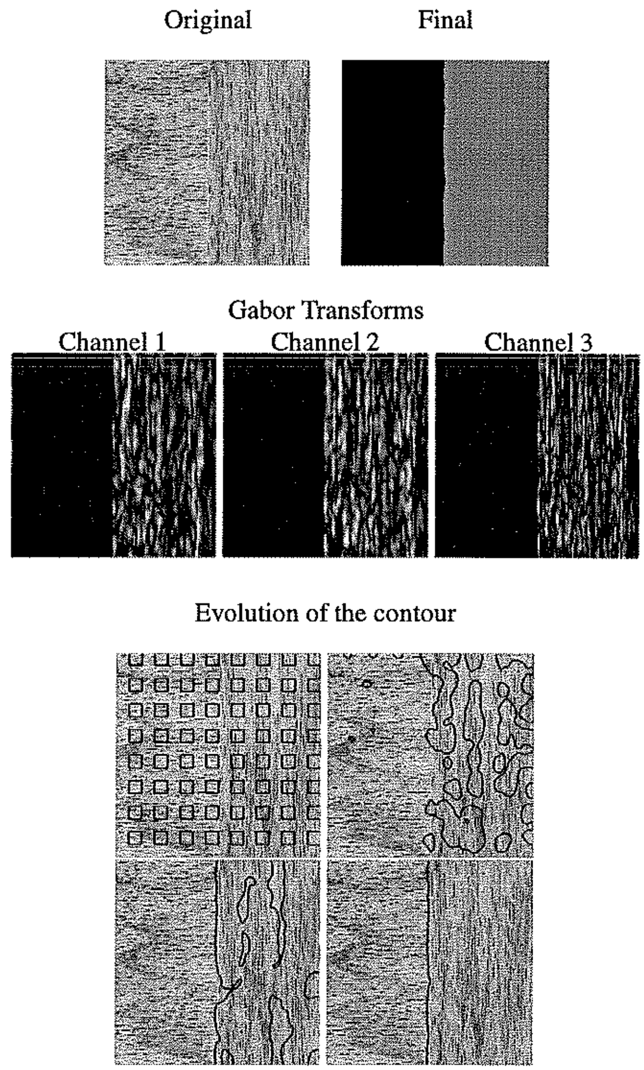

Figure 2: Supervised model with three active different Gabor transforms. Parameters: $\lambda_i = 1$, $\mu = 19500$, $\gamma_i = .3$. The boundary between the different angled textures is found. Note that we used a different initial contour, which allow for a faster result.

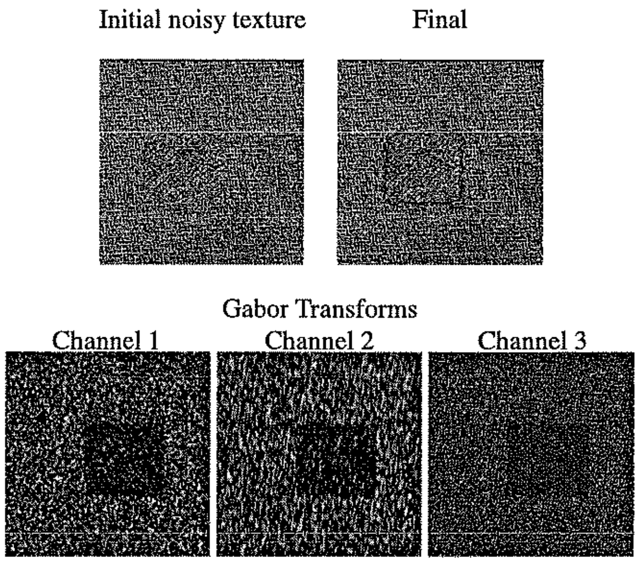

Figure 3: Supervised model with three active different Gabor transforms of an initial noisy textured image. Parameters: $\lambda_i = 1$, $\mu = 3000$, $\gamma_i = .5$. Eventhough the noise causes problems in the Gabor transforms, the model is able to find the square inside.

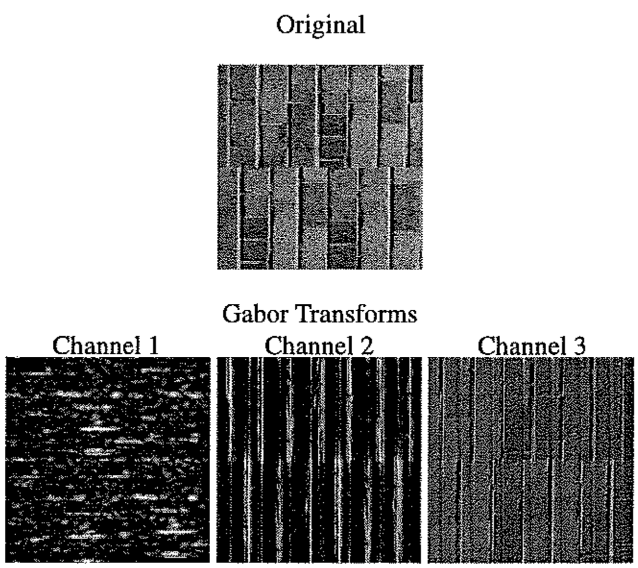

Figure 4: Supervised model with three different types of Gabor transforms that occured with this example. The model cannot find the boundary with any of the types of transforms found.

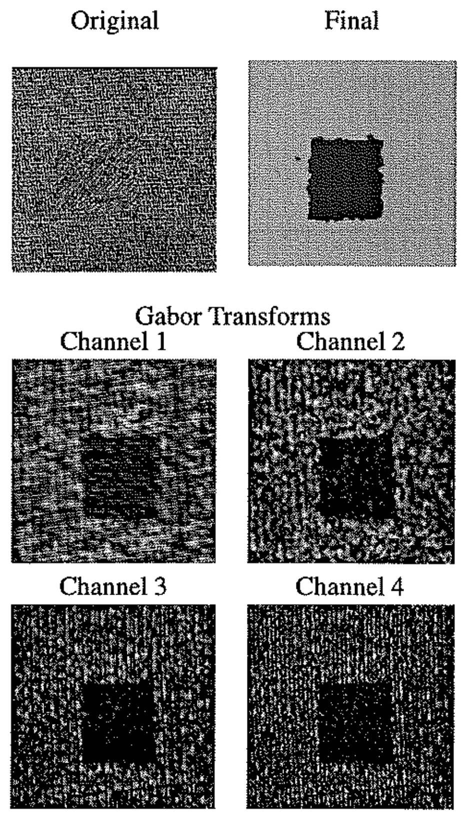

Figure 5: Unsupervised model with four active channels, chosen dynamically. We show here the final choice of the transforms. Parameters: $\lambda_i = 1$, $\mu = 3000$, $\gamma_i = .5$. The square is well detected.

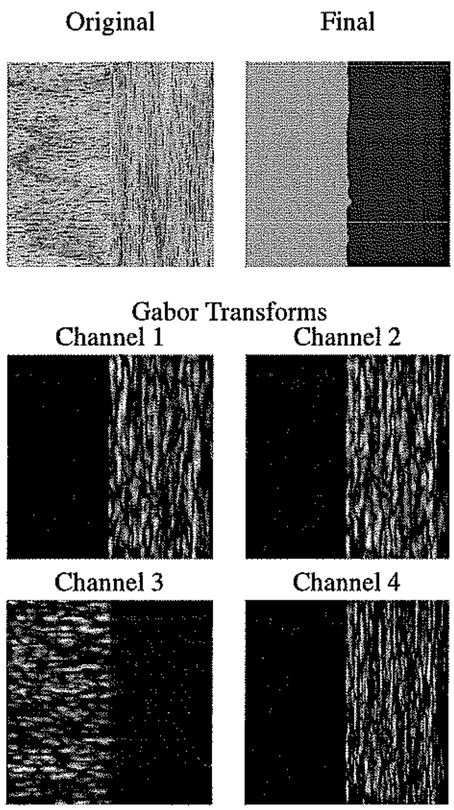

Figure 6: Unsupervised model with four active channels, chosen dynamically. We show here the final choice of the transforms. Parameters: $\lambda_i = 1, \mu = 19500, \gamma_i = .3$. The boundary between the different angled textures is found.

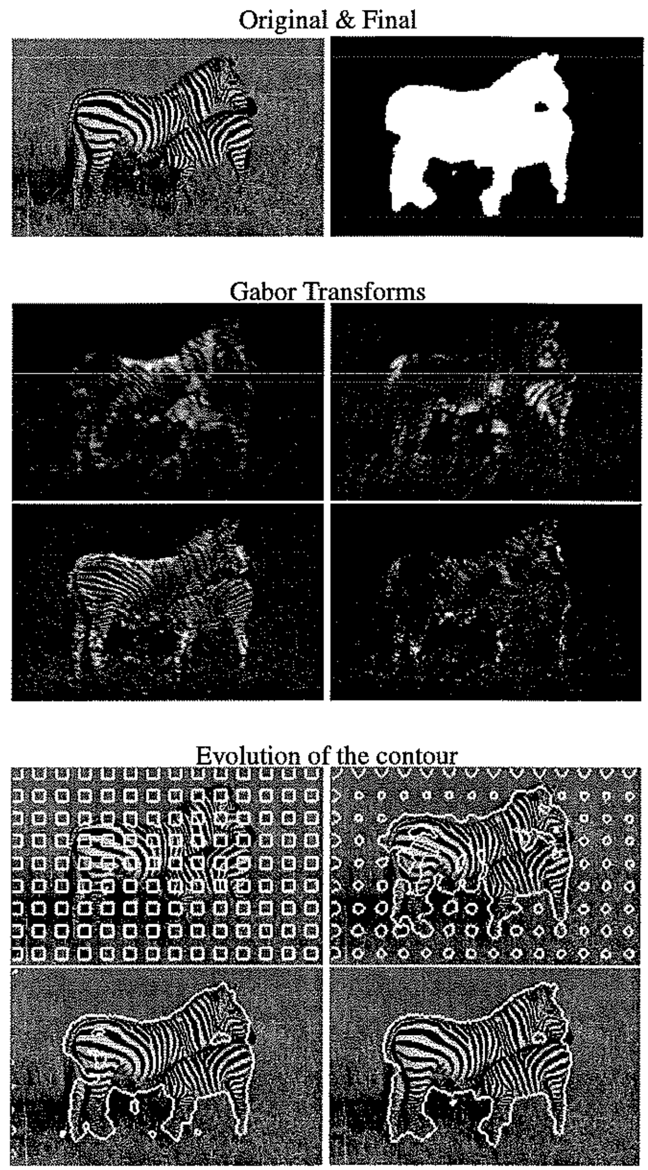

Figure 7: Supervised model for segmentation of the zebras image, with four active transforms.

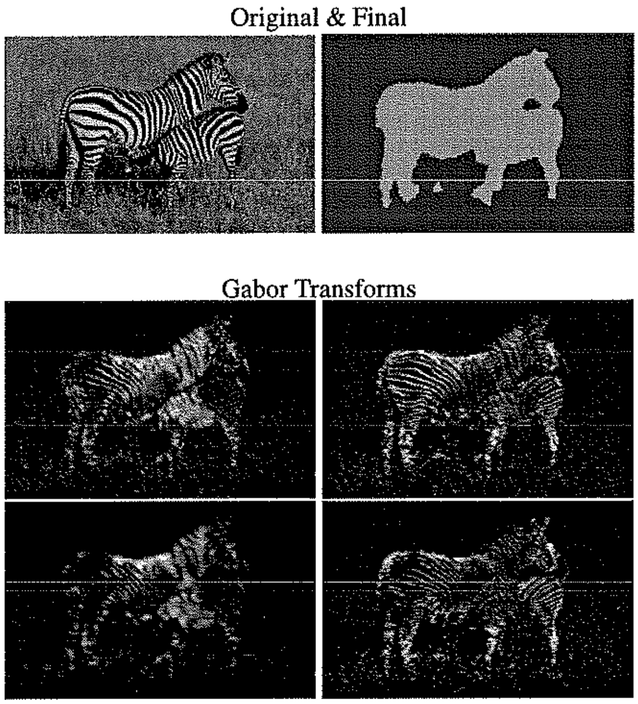

Figure 8: Unsupervised texture segmentation with only four active transforms. It is successful in segmenting the zebras and disregarding the stripes.

[9] D. Dunn, W. E. Higgins, J. Wakeley, "Texture Segmentation Using 2-D Gabor Elementary Functions", IEEE Transactions on Pattern Analysis and Machine Intelligence, Vol. 16, No.2, 1994.

[10] I. Fogel and D. Sagi, "Gabor Filters as Texture Discriminator", Biol. Cybern. Vol. 61, pp. 103-113, 1989.

[11] A. K. Jain, F. Farrakhonia, "Unsupervised Texture Segmentation Using Gabor Filters", Pattern Recognition, Vol. 23, No. 12, pp. 1167-1186, 1991.

[12] M. Kass, A. Witkin, and D. Terzopoulos, "Snakes: Active Contour Models", International Journal of Computer Vision, Vol. 1, pp: 321-331, 1988.

[13] S. Kichenassamy, A. Kumar, P. Olver, A. Tannenbaum and A. Yezzi, "Gradient flows and geometric active contour models", Proc. of ICCV, Cambridge, 1995, 810-815, 1995.

[14] G. Koepfler, C. Lopez, and J.M. Morel, "A multiscale algorithm for image segmentation by variational method", SIAM Journal of Numerical Analysis, Vol. 31:1, pp. 282-299, 1994.

[15] R. Malladi, J.A. Sethian, and B.C. Vemuri, "A Topology Independent Shape Modeling Scheme", Proc. SPIE Conf. on Geometric Methods in Computer Vision II, Vol. 2031, San Diego, pp. 246-258, 1993.

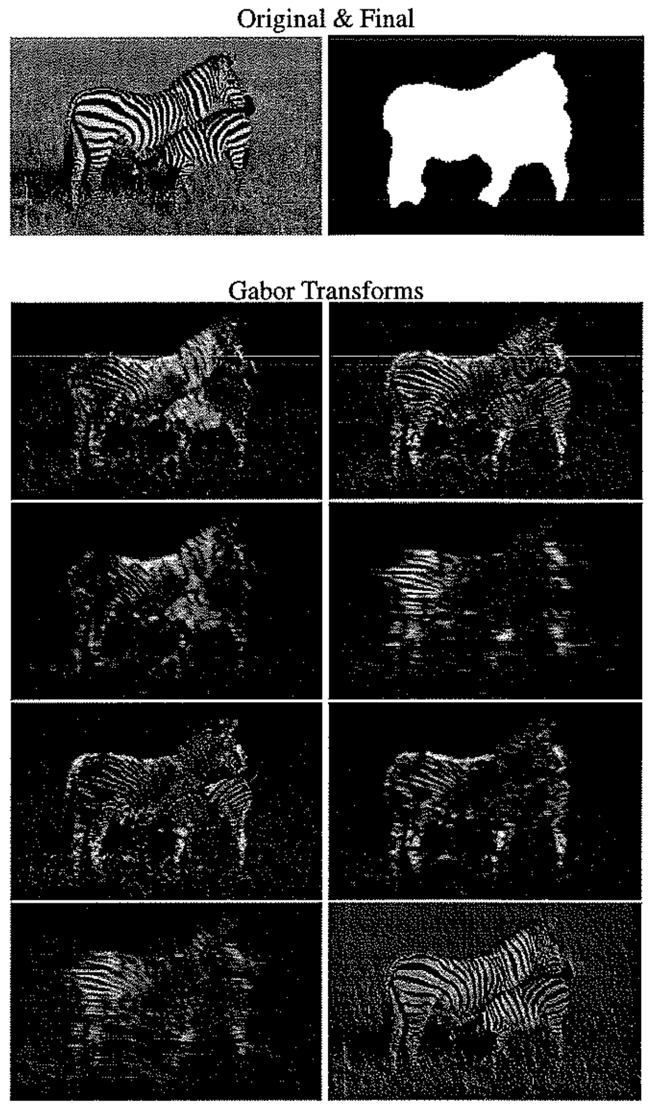

Figure 9: Unsupervised texture segmentation with eight active transforms. In this case adding more channels does not give any more information than with 4 channels.

[16] J. Malik, P. Perona, "A Computational Model of Texture Segmentation", *Proceedings of CVPR '89*, pp. 326-332, 1989.

[17] D. Mumford and J. Shah, "Optimal approximation by piecewise-smooth functions and associated variational problems", Commun. Pure Appl. Math., Vol. 42, pp. 577-685, 1989.

[18] S. Osher and J. A. Sethian, "Fronts Propagating with Curvature-Dependent Speed: Algorithms Based on Hamilton-Jacobi Formulation", Journal of Computational Physics, Vol. 79, pp. 12-49, 1988.

[19] N. Paragios, R. Deriche, "Geodesic active contours for supervised texture segmentation", Proceedings of the International Conference on Computer Vision and Pattern Recognition, June, Fort Collins, Colorado, 1999.

[20] N. Paragios and R. Deriche, "Geodesic Active Regions for Supervised Texture Segmentation", Proceedings of the 7th International Conference on Computer Vision, IEEE Computer Society Press, Kerkyra, Greece, 1999.

[21] Portilla J. and Simoncelli E.P., "A parametric texture model based on joint statistics of complex wavelet coefficients", IJCV, Vol. 40/1, pp. 49-71, 2000.

[22] G. Sapiro, "Color snakes", Computer Vision and Image Understanding, Vol. 68/2, pp. 247-253, 1997.

[23] G. Sapiro, "Vector (self) snakes: a geometric framework for color, texture, and multiscale image segmentation", Proc. IEEE ICIP, Vol. I, Lausanne, pp. 817-820, 1996.

[24] G. Sapiro, D. L. Ringach, "Anisotropic Diffusion of Multivalued Images", Lecture Notes in Control and Information Sciences, Vol. 219, M.-O. Berger, R. Deriche, I. Herlin, J. Jaffré and J.-M. Morel (Eds.), Proceedings of the 12th International Conference on Analysis and Optimization of Systems: Images, Wavelets and PDEs, Paris, (Springer), pp. 134-140, 1996.

[25] G. Sapiro and D. L. Ringach, "Anisotropic diffusion of multivalued images with applications to color filtering", IEEE Transactions on Image Processing, Vol. 5, pp. 1582-1586, 1996.

[26] K. Siddiqi, Y. B. Lauzière, A. Tannenbaum, and S.W. Zucker, "Area and Length Minimizing Flows for Shape Segmentation", IEEE Transactions on Image Processing, Vol. 7/3, pp. 433-443, 1998.

[27] P.H. Suen and Healey G., "The analysis and recognition of real-world textures in three dimensions", IEEE PAMI, Vol. 22/5, pp. 491-503, 2000.

[28] P.H. Suen and Healey G., "Modeling and classifying color textures using random fields in a random environment", Pattern Recognition, Vol. 32/6, pp. 1009-1017, 1999.

[29] D.-M. Tsai, S.-K. Wu, and M.-C. Chen, "Optimal Gabor filter design for texture segmentation using stochastic optimization", Image and Vision Computing, Vol. 19, pp. 299-316, 2001.

[30] T. P. Weldon, W. E. Higgins, "Design of Multiple Gabor Filters for Texture Segmentation", Proc. ISCAS, 1996.

[31] T. P. Weldon, W. E. Higgins, An Algorithm for Designing Multiple Gabor Filters for Segmenting Multi-Textured Images", IEEE Conference on Image Processing, Chicago, IL, Oct. 4-7, 1998.

[32] C. Xu, and J.L. Prince, "Snakes, Shapes and Gradient Vector Flow", IEEE Transactions on Image Processing, Vol. 7/3, pp. 359-369, 1998.

[33] H.K. Zhao, T. Chan, B. Merriman, and S. Osher, "A Variational Level Set Approach to Multiphase Motion", Journal of Computational Physics, Vol. 127, pp. 179-195, 1996.

[34] Zhu, S. C., Lee, T. S. and A. L. Yuille, "Region competition: Unifying snakes, region growing, Energy/Bayes/MDL for multi-band image segmentation", Proceedings of the IEEE 5th ICCV, Cambridge, pp. 416-423, 1995.

[35] Zhu, S. C. and A. Yuille, "Region competition: Unifying snakes, region growing, and Bayes/MDL for multi-band image segmentation", IEEE Transactions on Pattern Analysis and Machine Intelligence, Vol. 18, pp. 884-900, 1996.

[36] T. Chan and L. Vese, Active contours without edges, *IEEE Trans. Image Process.* [UCLA CAM Report 98-53] and An active contour model without edges, in *Proceedings of the Second Internaton Conference, Scale-Space '99. Corfu. Greece, September 26-27,1999* (M. Nielsen, P. Johansen, O. F. Olsen and J. Wieckert,Eds.) Scale-Space Theories in Computer Vision, 141-151.

[37] T. Chan, B.Sandberg, L. Vese, Active Contours without Edges for Vector-Valued Images, emphJournal of Visual Communication and Image Representation Vol. 11 pages 130-141.

[38] Tony Chan and L.A. Vese, Active Contour and Segmentation Models Using Geometric PDE's for Medical Imaging (invited paper), Malladi, R. (Ed.), "Geometric Methods in Bio-Medical Image Processing" Series: Mathematics and Visualization, Springer, 2002.

[39] L. Vese and T. Chan, A Multiphase Level Set Framework for Image Segmentation Using the Mumford and Shah Model, International Journal of Computer Vision, 2002 (in press).

[40] T.S. Lee, D. Mumford, and A. Yuille, Texture segmentation by minimizing vector-valued energy functionals - the coupled-membrane model, *L*ecture Notes in Computer Science, Vol. 588, pp. 165-173, 1992.

[41] S. Casadei, S. Mitter, and P. Perona, Boundary detection in piecewise homogeneous textured images, *L*ecture Notes in Computer Science, Vol. 588, pp. 174-183, 1992.

[42] C. Sagiv, N.A. Sochen, and Y.Y. Zeevi, Geodesic Active Contours Applied to Texture Feature Space, *M.* Kerckhove (Ed.): Scale-Space 2001, LNCS 2106, pp. 344-352, 2001.